Indian Journal of Pure & Applied Physics
Vol. 56, October 2018, pp. 759-764

Structural, optical and photovoltaic properties of Co (3%): CdZnS nanoparticles

Sabit Horoz*

Siirt University, Faculty of Engineering, Department of Electrical and Electronics Engineering, 56100, Siirt, Turkey

Received 11 December 2017; accepted 28 February 2018

In the present study, CdZnS and Co (3%): CdZnS nanoparticles (NPs) have been synthesized via wet chemical method at room temperature using 1-thioglycerol as a capping agent. The incident photon-to-current conversion efficiency (IPCE) measurement has been carried out for Co (5%): CdZnS for the first time in this study. The results show that Co (3%): CdZnS can be utilized as sensitizers to improve the performance of solar cells. In addition to the photovoltaic properties; structural, optical and morphological properties of Co (3%): CdZnS NPs have been investigated. The results indicate that Co (3%): CdZnS NPs can be suitable material for photovoltaic applications.

Keywords: Characterizations, Co-doped CdZnS, Nanoparticles, Photovoltaic properties, Wet-chemical method

1 Introduction

Wide bandgap metal chalcogenide group II-VI semiconductor nanoparticles (NPs) have been extensively used in due to their unique optical properties, optoelectronic applications such as solar cells, sensors, blue lasers, and light emitting diodes (LEDs)[1-4]. The band gap of the NPs is able to be controlled by changing the particle size. The situation is identified as a feature of the quantum confinement effect. Hence, the energy levels become discrete so that the band gap increases when the particle size becomes smaller[5].

Among these group of II-VI semiconductor, ZnS and CdS chalcogenides have a direct bandgap of 3.6 and 2.24 eV at room temperature, respectively and these have been widely studied as important materials for optoelectronics and energy applications[6,7]. Cadmium zinc sulfide (CdZnS) NPs which are synthesized using appropriate Cd:Zn ratio, have been broadly employed as capable wide band gap semiconductors for manufacturing hetero-junction solar cell devices[8,9]. The CdZnS, a ternary chalcogenide semiconductor, has a wider bandgap (2.4 – 3.7 eV) than CdS (2.24 eV). Mitchell *et al.*[10] and Torres *et al.*[11] reported that due to the fact that CdS is replaced by CdZnS NPs, it could block the window absorption losses and rise in the short-circuit current. Additionally, the CdZnS is able to be utilized as a window material for construction of *p-n* junctions without lattice mismatch in devices[12].

Doped semiconductors NPs, diluted magnetic semiconductors (DMS), are a new class of luminescent materials for applications of nanocomposite materials with new opportunities for research[13]. Transition metals such as manganese (Mn), nickel (Ni) and cobalt (Co) have been generally used as dopants[14-16]. Even though there are many studies on the ferromagnetic properties of Co- doped CdS and ZnS NPs[17,18], there are no reports on room temperature ferromagnetism in Co-doped CdZnS NPs. As a result of motives such as (*a*) Co metal is ferromagnetic having high magnetic moment (*b*) theoretical investigation similarly provides the scene of fabricating ferromagnetism in Co-based semiconductors, Co has been picked as a dopant in this study.

From the application point of view, CdS and ZnS NPs doped with transition ions have been studied as an alternative strategy to boost the efficiency of solar cells because they create long–lived photo generated charge carriers, reduce the electron-hole recombination, and have a long lifetime and facilitate the charge transfer from the NPs to the photoelectrode[19,20]. Zhou *et al.*[21] reported that the CdS/Co-Doped-CdSe cell exhibits the photovoltaic performance with power conversion efficiency (η) of 0.89%. However, no work was found about solar cell application of Co-doped CdZnS NPs. For this reason, this study will be original.

In this study, the synthesis and characterizations of CdZnS and Co (3%): CdZnS NPs have been reported, prepared by the wet-chemical method at room

*E-mail: sabithoroz@siirt.edu.tr

temperature using the using 1-thioglycerol as a capping agent. Their structural, optical, and magnetic properties have been studied. Moreever, the effect of Co dopant on the performance of CdZnS solar cells have been investigated. Till date, no reports have been observed on photovoltaic properties of Co-doped CdZnS NPs.

2 Experimental Part

2.1 Materials

Commercial $Cd(CH_3COO)_2.2H_2O$ as Cd source, Zn $(CH_3COO).2H_2O$ as Zn source, $Co(CH_3COO)_2{\cdot}4H_2O$ as Co source and Na_2S as S source, were of analytical grade and were used without further purification to synthesize CdZnS and Co (3%): CdZnS nanoparticles (NPs)at room temperature using co-precipitation method. 1-thioglycerol ($C_3H_8O_2S$) was used as a capping agent to prevent any agglomeration during the preparation.

2.2 Preparation

For synthesis of un-doped CdZnS;0.5 M aqueous solutions of Cd $(CH_3COO)_2.2H_2O$, 0.025 M aqueous solutions of Zn $(CH_3COO).2H_2O$ and 0.5 M aqueous solutions of Na_2S were dissolved into three different beakers. These three solutions cation and anion sources were transferred into fourth clean beaker and stirred at certain time to get homogeneous mixture of CdZnS at room temperature. While stirring, the 1-thioglycerol (0.5 mL) was added onto the mixture. The percipated sample was seperated from the solution by a filter paper. De-ionized water and ethanol were used to wash the resultant particles to get rid of unwanted compounds inside the particles. The obtained final solution was heated in oven at 80 °C. Orange colour of CdZnS NPs were obtained after grinding the powders using a mortar.

For synthesis of Co(3%) doped CdZnS NPs; 0.015 M aqueous solutions of $Co(CH_3COO)_2{\cdot}4H_2O$ was added onto the solution of [0.5 M Cd $(CH_3COO)_2.2H_2O$ and 0.025 M Zn $(CH_3COO).2H_2O$], seperately then, followed the same procedure as mentioned above.

2.3 Characterization

X-ray diffraction (XRD) on a Rigaku X-ray diffractometer with Cu K_α (λ= 154.059 pm) radiation were used to characterize the structural properties of the samples. UV-VIS absorption spectra were recorded using a Perkin- Elmer Lambda 2 spectrometer. Photoluminescence (PL) measurement was carried out with a Perkin-Elmer LS 50B at room temperature, using 310 nm as the excitation wavelength. Incident photon-to-current conversion efficiency (IPCE) measurements was performed by using PCE-S20 with a monochromatic light source consisting of a 150-W Xe lamp and a monochromator. For the IPCE measurements, fluorine doped tin oxide (FTO, $13\Omega.sq^{-2}$) conductive glass substrates were used as the photo electrodes. The TiO_2 nanowires (NWs) were coated on the FTO substrates using the doctor blade method, then sintered at 450 °C for 45 min. A suspension of un-doped and Co (3%) doped CdZnS NPs were dropped on the FTO substrates with the TiO_2 NWs. The substrates were dried with N_2 gas and secured against Cu_2S counter electrodes containing polysulfide electrolytes.

3 Results and Discussion

3.1 Structural properties

The XRD patterns of CdZnS and Co (3%): CdZnS NPs are indicated in Figure 1. It can be clearly seen that all the diffraction peaks of NPs, can be well indexed as the zinc blende (cubic) phase structure of CdS, which are consistent with the standard card (JCPD No: 65-2887).

It was observed that the three diffraction peaks correspond to the lattice planes of (111), (220) and (311), respectively, suggesting that the Co content has been incorporated into the CdZnS lattice. The XRD patterns demonstrate that the full width at half height maximum (FWHM) of the diffraction peaks of CdZnS

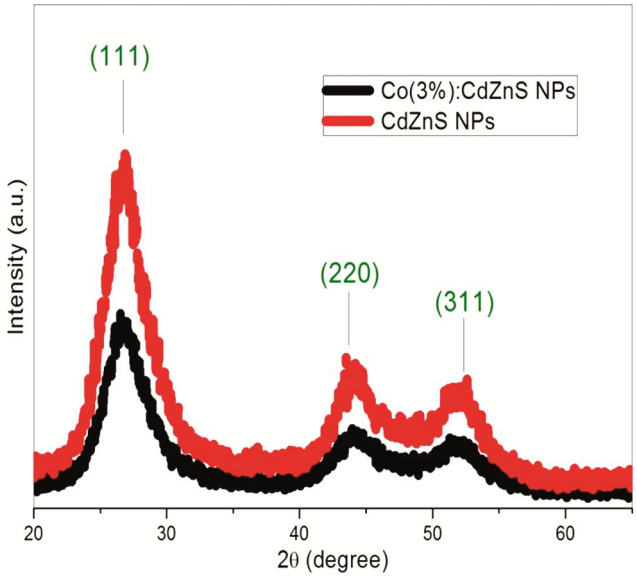

Fig. 1 – X-ray diffraction patterns of CdZnS and Co (3%): CdZnS NPs prepared at room temperature.

NPs increases with doping which results in the degradation and decreases in the crystallite size. Based on the FWHM, the average particle sizes (*PS*s) of CdZnS and Co (3%): CdZnS NPs, were calculated using the Debye-Scherrer equation, $PS=0.9\lambda/(\beta\cos\theta)$; where λ=0.15418 nm, is the X-ray wavelength provided from a Cu (α) radiation, β is the FWHM in radians and θ is the Bragg's angle, are 2.61 and 2.57 nm, respectively. The Co^{2+} ions occupy the regular lattice site of Cd^{2+} ions that what may be possible reason for the decrease in the crystallite size. Moreover, this ion substitution could cause the crystal defects and charge imbalance in CdZnS structure.

3.2 Optical properties

We investigated the optical properties and analyzed the energy band gap of CdZnS and Co (3%): CdZnS NPs by UV-visible absorption spectroscopy. Crystal imperfection may occur due to the dopant which changes the bandgap of the semiconductor. Figure 2 reveals the optical absorption spectra of CdZnS and Co (3%): CdZnS NPs in the wavelength range 300–800 nm.

Some factors such as particle size and defects in the structure can change the absorbance of the samples. The UV-Vis absorption spectra show the ultraviolet cut-off absorption of Co (3%): CdZnS NPs shifts to higher energy (shorter wavelength) compared with CdZnS. The absorption edge is found to shift towards shorter wavelengths (blue shift) which mean the band gap increases which may be caused by crystallite size owing to the doping.

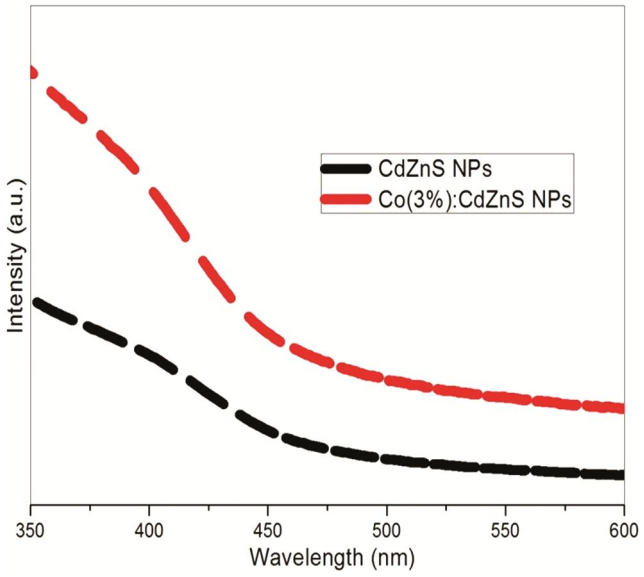

Fig. 2 – UV-Vis absorption spectrums of CdZnS and Co (3%): CdZnS NPs prepared at room temperature.

The Tauc relation is given in Eq. (1), were used to calculate the energy band gap (E_g) of the NPs.

$$\alpha h\upsilon = C(h\upsilon - E_g)^n \quad ...(1)$$

Where α is the absorption coefficient, n=1/2 or 2 for direct or indirect allowed transition, respectively, C is the characteristic parameter for respective transitions, $h\upsilon$ is photon energy and E_g is energy band gap. Plots of $(\alpha h\upsilon)^2$ versus $h\upsilon$ for CdZnS and Co (3%): CdZnS NPs are shown in Fig. 3.

As can be seen in Fig. 3, the band dap of CdZnS NPs, has a large band gap (3.79 eV), increases with Co content. The blue shift in the absorption edge is due to the quantum confinement of the excitons present in the sample, causing a more discrete energy spectrum of the individual NPs. Using Brus's equation is given in earlier study[22], the particle sizes for CdZnSand Co (3%): CdZnS NPs were calculated. Table 1 indicates the band gap and size calculation for samples.

It was found that the Co content results in the reduction in size of CdZnS NPs which clearly relates to an increase in the bandgap value. The reason for this could be owing to the quantum confinement effect on the bulk of CdS. The effect of the quantum confinement on impurity depends upon the size of the

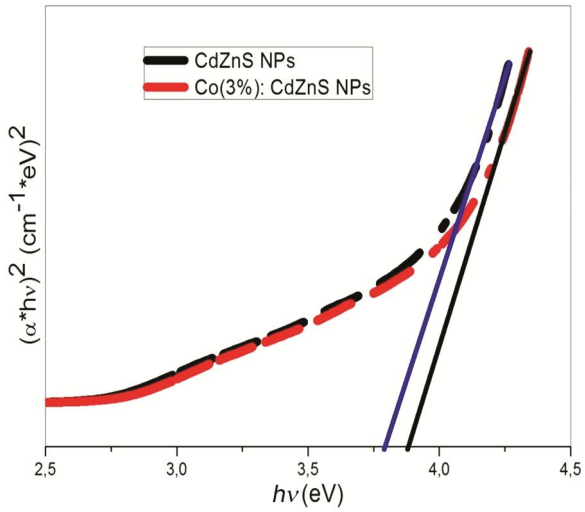

Fig. 3 – Determination of the optical band gap of CdZnS and Co (3%): CdZnS NPs prepared at room temperature using $(\alpha h\upsilon)^2$ versus $h\upsilon$ plot.

Table 1 – Particle size and bandgap variation with Co content.

Sample (NPs)	Band gap energy (eV)	Particle size (nm)
CdZnS	3.79	2.40
Co (3%): CdZnS	3.88	2.34

host crystal. The obtained sizes for CdZnS and Co (3%): CdZnS NPs are in good agreement with the results from XRD analysis.

The optical properties of semiconducting NPs are explored by photoluminescence (PL) which is a perceptive helpful method[23]. It gives us information about the energy states of impurities and defects, yet at very low densities, for understanding structural defects, the crystallinity, surface defects, energy bands and exciton fine structure. The defects like sulfur vacancies in grain boundaries and the presence of doping atoms in the surface and intergranular layers which affect some physical properties such as optical properties of nano-sized metal sulfide materials[24].

Figure 4 demonstrates the room temperature PL excited with a wavelength of 310 nm for CdZnS and Co (3%): CdZnS NPs in the wavelength range 492-800 nm.

It is seen that whereas the CdZnS NPs has only one green emission band centered at 510.7 nm, which is related to radiative recombination involving defect states in the CdZnS NPs, Co (3%): CdZnS NPs has a broad emission peak at 583 nm. Compared with the PL spectrum of CdZnS NPs, the spectra of Co (3%): CdZnS NPs are slightly red-shifted in the similar size regime. The shift in the PL spectra could be due to fact that the initial Co- doping induces defects because of self-concentration.

3.3 Morphological properties

The shape and morphology properties of CdZnS and Co (3%): CdZnS NPs were investigated by SEM analysis. Figure 5(a, b) indicates typical SEM images of CdZnS and Co (3%): CdZnS NPs, respectively. It was observed that CdZnS and Co (3%): CdZnS NPs have tightly packed surface morphology and this result is consistent with the study done by Theerthagiri *et al.*[25] They synthesized CdZnS nanocrystals and reported that composite materials have tightly packed surface morphology. It was also notified that this condition is useful for charge carrier separation and solar cell devices.

The energy dispersive X-ray (EDX) spectrum was used to confirm the elemental compositions of CdZnS and Co (3%): CdZnSNPs. The peaks obtained from the EDX spectra for CdZnS and Co (3%): CdZnS NPs are shown in Fig. 6(a, b) respectively, which are associated with Cd, Zn, S and Co. The obtained EDX results proved that Co content was successfully doped into CdZnS NPs.

3.4 Photovoltaic properties

The charge generation and collection of the solar cell can be evaluated by incident photon-to-current

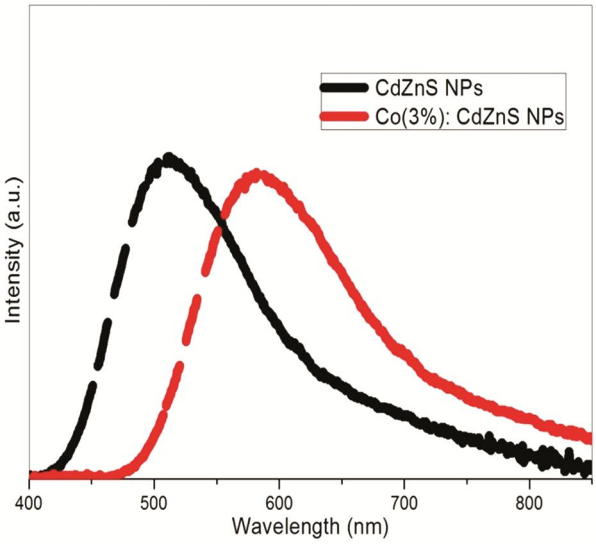

Fig. 4 – Photoluminescence (PL) spectra at room temperature excited with a wavelength of 310 nm (4.0 eV) forCdZnS and Co (3%): CdZnS NPs prepared at room temperature.

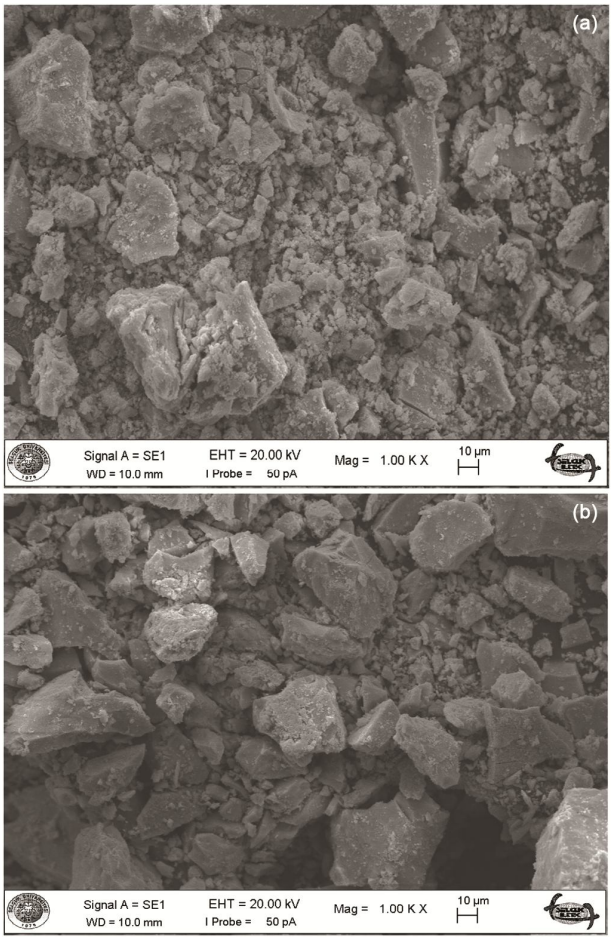

Fig. 5 – SEM image of (a) CdZnS and (b) Co (3%): CdZnS NPs.

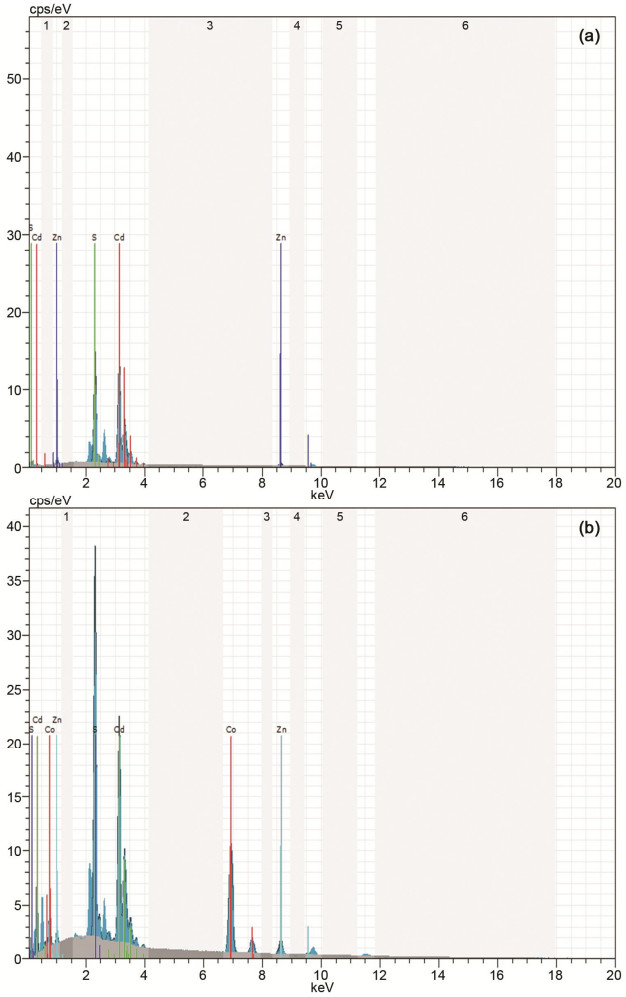

Fig. 6 – EDX spectrum of (a) CdZnS and (b) Co (3%): CdZnS NPs.

conversion efficiency (IPCE). The IPCE measurement for Co (3%): CdZnS NPs was carried out for the first time in this study. The IPCE spectra of CdZnS and Co (3%): CdZnS NPs that were subsequently attached on TiO_2 nanowires (NWs)at different incident light wavelengths are indicated in Fig. 7.

Based on Fig. 7, two observations were obtained. One of is that the value of the IPCE becomes better with NPs which have smaller particle size. The IPCE value was about 11 % at 400 nm observed for Co (3%): CdZnS NPs followed by 7.5% for the CdZnS NPs. The second is that the spectral response range of Co (3%): CdZnS NPs is wider than CdZnS NPs. The reason for this situation is that the introduction of impurities of dopant enhances the spectral response of the NPs. Hence, more electrons transferred to the external circuit and the generation of dark current is also suppressed.

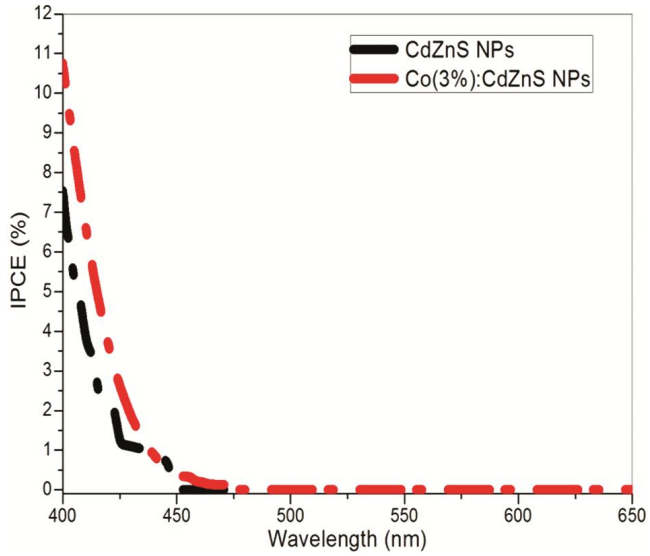

Fig. 7 – Comparison of the IPCE spectra of CdZnS and Co (3%): CdZnSNPs attached on the TiO_2 NWs.

4 Conclusions

In this study, the structural, optical, morphological and photovoltaic properties of CdZnS and Co (3%): CdZnS NPs, prepared by the co-precipitation method at room temperature using 1-thioglycerol as a capping agent as a capping agent, were investigated. Study (XRD) on the structural properties showed that CdZnS and Co (3%): CdZnS NPs have cubic (zinc blende) structure and the particle size of CdZnS NPs doped by Co becomes smaller than CdZnS NPs. The optical absorption spectra revealed that the absorbance of Co (3%): CdZnS NPs are blue shifted compare to CdZnS NPs. It means that the band gap increases which may be caused by crystallite size as the doping concentrations increase. It was also observed the red-shift in PL of Co (3%): CdZnS NPs compares with the PL spectrum of CdZnS NPs. The shift in the PL spectra could be due to fact that the initial Co- doping induces defects because of self-concentration. The IPCE measurement was carried out for Co (3%): CdZnS NPs for the first time in this study. The IPCE value was about 11 % at 400 nm observed for Co (3%): CdZnS NPs followed by 7.5% for the CdZnS NPs. Moreover, the IPCE measurement showed that the spectral response range of Co (3%): CdZnS NPs is wider than CdZnS NPs. Consequently, results obtained from the IPCE measurements revealed that Co (3%): CdZnS NPs can be utilized as sensitizers to improve the performance of solar cells.

References

1 Ziabari A A & Ghodshi F E, *Solar Ener MaterSolar Cells*, 105 (2012) 249.
2 Saravanan R S S, Pukazhselvan D & Mahadevan V, *Philos Mag*, 91 (2011) 389.
3 Zhong X, Feng Y, Knoll W & Han M, *J Am Chem Soc*, 125 (2003) 13559.
4 B J Wu, Cheng H, Guha S, Haase M A, Depuydt J, Meishaugen G & J Qui, *Appl Phys Lett*, 63 (1993) 2935.
5 Nath S S, Chakdar D, Gope G, Talukdar A & Avasthi D K, *Philos Mag*, 30 (2009) 1111.
6 Yamamoto T, Kishimoto S & Ilida S, *Phys*, 308 (2001) 916.
7 Khosravi A A, Bigdeli F B, Yousefi M, Abdikhani M S & Otaqsara S M T *Environ Prog Sust En*, 33 (2014) 1194.
8 Salem A M, *Appl Phys* A, 74 (2002) 205.
9 Kim S Y, Kim D S, Ahn B T & Im H B, *J Mater Sci Mater Electron*, 4 (1993) 178.
10 Mitchell K W, Fahrenbruch A L & Bube R H, *J Appl Phys*48 (1977) 4365.
11 Torres J & Gordillo G, *The Soul Film*, 207 (1992) 231.
12 Walter T, Ruckh M, Velthaus K O, Schock H W, *Proc of the 11th EC Photovol Sol En Conf*, (1992) 124.
13 Liu H, Fei L, Liu H, Lang J, Yang J, Liu Y, Gao M, Liu X, Chen X & Wei M, *J Alloys Comp*, 587 (2014) 222.
14 Horoz S, Dai Q, Maloney F S, Yakami B, Pikal J M, Zhang X, Wang J, Wang W & Tang J, *Phys Rev Appl*, 302 (2015) 4011.
15 Kumar R S, Veeravazhuthi V, Muthukumarasay N, Thambidura M & Shankar D V, *Super Micr*, 86 (2015) 552.
16 Zhao W, Wei Z, Zhang L, Wu X, Wang X & Jiang J, *J Alloys Comp*, 698 (2017) 754.
17 Lavanya T, Satheesh K & Jaya N V, *IOP Conf Series: Mat Sci Eng*, 73 (2017) 012114.
18 Sambasivam S, Joseph D P, Lin J G & Venkateswaran C, *J Solid State Chem*, 182 (2009) 2598
19 Santra P K & Kamat P V, *J Am Chem Soc*, 134 (2012) 2508.
20 Horoz S & Sahin O, *J Mat Sci: Mat Elect*, 28 (2017) 9559.
21 Zou X, He S, Teng G & Zhao C, *J Nanomater*, (2014) 818160.
22 Brus L, *J Phys Chem*, 90 (1986) 2555.
23 Hassan M H, Khan W, Azam A & Naqvi A H, *J Lumin*, 145 (2014) 160.
24 Shen S & Wang Q, *Chem Mat*, 25 (2013) 1166.
25 Theerthagiri J, Senthil R A & Madhavan J, *Mat Sci For*, 832 (2015) 158.